

## Original Article

# Dynamic transcriptome landscape of pulmonary tissues of rats infected with *Paragonimus proliferus*

Guoji Chang<sup>1\*</sup>, Na Li<sup>2\*</sup>, Qingqing Wang<sup>1\*</sup>, Jie Ding<sup>1</sup>, Siqi Liu<sup>1</sup>, Lijuan Hua<sup>1</sup>, Shenghao Li<sup>1</sup>, Wenlin Wang<sup>3</sup>

<sup>1</sup>Clinical-Medical Center of Infectious Disease of Yunnan Province, The Third People's Hospital of Kunming, Kunming 650043, Yunnan, China; <sup>2</sup>Department of Pharmacy, The Third People's Hospital of Kunming, Kunming 650043, Yunnan, China; <sup>3</sup>School of Basic Medicine, Kunming Medical University, Kunming 650504, Yunnan, China. \*Equal contributors.

Received December 28, 2021; Accepted April 30, 2022; Epub May 15, 2022; Published May 30, 2022

**Abstract:** Paragonimiasis (pulmonary fluke disease) is a foodborne parasitic disease caused by trematode infections. *Paragonimus proliferus* is a characteristic *Paragonimus* species that was first identified in Yunnan Province of China. No direct evidence has yet proven that *P. proliferus* can infect humans. However, we previously found that *P. proliferus* infects and damages rat lung tissues via an unclear mechanism. Here, we infected Sprague Dawley rats with *P. proliferus* and sequenced their lung transcriptomes at various intervals thereafter. We detected *P. proliferus* on the surface of rat lung tissues at 7 days post infection. It colonized by attaching and secreting dsRNA and utilized nutrients from the lung tissues for mitosis and meiosis and the dynein arm of lung tissues to develop symmetrical organs. The rats generated different types of immune responses that differed according to the stage of infection. We then analyzed *P. proliferus* responses to these immune strategies and the genes expressed during each stage of infection. Our findings provide a foundation for developing medical treatments for *P. proliferus* infection.

**Keywords:** *Paragonimus proliferus*, sprague-dawley rats, transcriptome sequencing

## Introduction

*Paragonimus* (Trematoda: Paragonimidae) is a mammalian parasite that causes paragonimiasis (lung fluke disease), which is a representative of zoonotic foodborne type of helminthiasis that occurs worldwide [1]. Humans can be infected with *Paragonimus* by eating raw freshwater crustaceans, mostly crayfish or crabs. Over 50 *Paragonimus* species have been identified globally, particularly in China [2]. *Paragonimus* infection causes inflammation of the infected site and increased serum eosinophil levels in host [3]. Numerous inflammatory cells then aggregate and undergo necrosis, which results in the fibrosis of surrounding tissues. Adult worms survive and lay eggs in mucous abscess cavities. The eggs stimulate the formation of chronic granulomas and eventually form tissue masses [4, 5]. The imaging and clinical manifestations of *Paragonimus* infection are similar to those of tuberculosis and tumors, thus causes misdiagnoses and delayed

treatment, resulting in respiratory failure, liver cirrhosis, epilepsy, blindness, and death [6].

*Paragonimus proliferus* was first found in Yunnan province of China. However, little is known about its morphology, genetic evolution, and pathogenicity. Within the genus *Paragonimus*, the formation of *P. proliferus* metacercariae differs from that of other *Paragonimus* spp. in their second intermediate host, crabs [7]. Zhou et al. [8] has provided a detailed morphological description of *P. proliferus* worms and eggs. The genetic evolution of the worm was also determined using ITS2 and CO1 gene sequences; parasites in Lüchun County (Yunnan, China) are highly homologous and belong to the same species. *Paragonimus proliferus* has been identified in Quang Binh (Central Vietnam) and its genome has been sequenced [9]. The ITS2 genes of parasites were 100% homologous between Laizhou (Northern Vietnam) and Fenggong (Yunnan, China), with a 5.6% gene mutation rate, sug-

gesting that *P. proliferus* is distributed in nature.

We previously found that intraperitoneal and subcutaneous injections of metacercariae cysts into the abdominal wall can infect experimental rats and result in lung damage. Li [10] investigated dynamic changes in tissue inhibitor matrix metalloproteinase 1 (*TIMP-1*) and matrix metalloproteinase 9 (*MMP-9*) expression in rats infected with *P. proliferus* and found that they induced lung fibrosis. Lung lesions are associated with the infection period and expression levels of *TIMP-1* and *MMP-9*, suggesting that *TIMP-1* and *MMP-9* play important roles in lung fibrosis in rats. The mechanisms of pathogenesis, immune evasion, and organ localization in hosts infected by *P. proliferus* have remained obscure, which has hampered further exploration of the prevention and treatment of paragonimiasis.

Here, we compared Sprague-Dawley (SD) rats infected with *P. proliferus* metacercariae with healthy control SD rats. We sequenced RNA in rat lung tissues at various intervals after infection to detect differentially expressed genes (DEGs). We also assessed the functional enrichment of DEGs and co-expression modules to reveal the parasitic profile of *P. proliferus* and reaction pathways. We then determined the immune responses of the rats at various stages of infection. Our findings could provide a deeper understanding of the pathogenic mechanism of *P. proliferus* and facilitate the development of novel medical therapies.

### **Materials and methods**

#### *Parasite materials*

We obtained freshwater crabs infected with *P. proliferus* metacercariae from the ponds in Xishuangbanna Autonomous Prefecture (previously called Jinghong County) and isolated metacercariae as described [11]. The metacercariae were then counted using a stereomicroscope and stored at 4°C.

#### *Animal model*

We obtained 60 male SD rats weighing 200 ± 30 g and fed them separately. Ten uninfected rats comprised a control group. Each of the remaining 50 rats was infected with eight *P.*

*proliferus* metacercariae via subcutaneous injection at abdominal wall. The infected rats were divided into five groups that were analyzed at 3, 7, 14, 28, and 70 days postinfection (dpi). Rats were sacrificed by anesthesia with 2% pentobarbital (i.p.) with a dose of 0.3 ml per 100 g on 3, 7, 14, 28, and 70 dpi and lung tissues were extracted and stored at -80°C.

#### *HE staining of rat lung tissues and semi-quantitative histopathological analysis*

Rat lung tissues were stained with hematoxylin & eosin (HE) at each time point. In order to more accurately assess the histological pathology of the lungs, according to the methods reported by Szapiel et al. [12], a semi-quantitative histopathological analysis of the stained slices were performed. HE-stained sections were scored via the following criteria: A score of 0 means no alveolitis; a score of 1 point represents mild inflammation, with manifestations like thickened alveolar walls, infiltration of inflammatory cell with involvement limited to focal, tissue lesions in less than 20% of the lung with well-preserved structures of the alveolar; 2 points mean moderate alveolitis, involving 20-50% of the lung; 3 points represent severe lesions of lung tissues which occupied more than 50% of the lung, even with extensive lung consolidation of air spaces due to alveolar swelling, destruction and inflammatory cell infiltration. Three biological replicates were prepared at each time point, and 5 tissue sections were taken from each tissue sample for HE staining. Finally, 15 pathological scores were obtained at each time point for statistical analysis. One-way ANOVA was then used for statistical analysis using SPSS 20.0 software. The final pathological scores for each time point were expressed as mean ± standard deviation, and  $P < 0.05$  was considered statistically significant.

#### *RNA sequencing*

We sequenced total RNA to clarify gene expression in the lung tissues of infected rats. Total RNA was extracted using TRIzol (Invitrogen, Carlsbad, CA, USA) [13], quantified using a NanoDrop ND-1000 (Thermo Fisher Scientific Inc., Waltham, MA, USA), and then resolved by gel electrophoresis. Thereafter, we constructed a sequencing library using total RNA (1 µg) with

the TruSeq RNA library preparation kit according to low-throughput instructions (Illumina Inc., San Diego, CA, USA). However, in contrast to the protocol, we prepared first-strand cDNA using SuperScript III reverse transcriptase (Invitrogen). After PCR enrichment and purification, the DNA concentration in the library was evaluated by qRT-PCR using an Applied Biosystems™ 7,500 Real Time PCR system (Thermo Fisher Scientific Inc.). We then sequenced the RNA library using the Illumina HiSeq 2500 system (Illumina) [14].

### *Quality control and read mapping*

We obtained high-quality clean data by filtering low-quality reads (including those containing adaptors with quality scores < 20, and base rates > 10%) using Sickle (<https://github.com/najoshi/sickle>) and SeqPrep [15]. The clean reads were aligned with the mouse reference genome (GRCm38.p5, Ensembl v. 86) using Bowtie2 [16].

### *Identification of differentially expressed genes*

Gene expression was quantified using the RNA-Seq by Expectation-Maximization (RSEM) tool [17], and DEGs between infected and control rats were selected using the R package NOISeq. We excluded false-positive DGEs by correcting *P* values using the Benjamini and Hochberg method. We adopted a negative binomial distribution statistical approach to normalize the sequenced data. We defined genes with a fold change (FC) ≥ 2, degree of expression ≥ 1, and probability ≥ 0.8.

### *Functional enrichment analysis of DEGs*

We annotated the DEGs by Gene Ontology (GO) using DAVID (<https://david.ncifcrf.gov/>), and assessed their GO enrichment using hypergeometric tests of the entire genome [18]. Values for GO terms with *P* < 0.05 were considered significantly enriched.

### *Quantitative real-time polymerase chain reaction (qRT-PCR)*

We validated selected DEGs by qRT-PCR using FastQuant RT Kits to reverse-transcribe mRNA and an ABI 7500 Real-time PCR Detection System with SuperReal PreMix Plus (Thermo Fisher Scientific Inc.). Relative gene levels were determined using the  $2^{-\Delta\Delta C_t}$  method.

## Results

### *Histopathological changes in lung tissues of infected rats*

Sprague-Dawley rats were infected *via* subcutaneous injection of cercariae obtained from crabs. The cercariae migrated to the surfaces of lung tissues and formed a slightly inflamed and bleeding lesion by 7 dpi. The body of the worms became black and slightly increased in size. The uterus, ovaries, and testicles of the worms began to develop by 14 dpi. The numbers of inflamed and bleeding lesions increased in the lungs, and some lung tissues became darkened. Fully developed uterus, testicles, and ovaries indicated that the worms had matured by 28 dpi. The infected lungs were severely damaged with large and blackened areas, adhesions, bleeding, edema, and pleural effusion. Capsules with thin, soft walls were evident. Wheeze, cough, hemoptysis, shortness of breath, and malaise were obvious, and many rats died at  $28 \pm 7$  dpi. The capsule walls were thick and stiff and the numbers of capsules increased by 70 dpi. Inflammation of the peripheral lung tissues improved, and some lung tissues adhered. The distinguishing features of the infected rat lungs indicated that the entire parasitic process comprised initial infection followed by early-, mid-, and post-parasitic periods (0-7, 8-28, and ≥ 29 dpi, respectively). **Figure 1** shows the lungs, parasitic worms, rat lung tissues stained with HE at each time point, and semi-quantitative histopathological analysis.

### *RNA sequencing of lung tissues of rats at various infection stages*

Three infected rats were sacrificed at 0, 3, 7, 14, 28, 70 dpi and lung tissues were isolated for RNA sequencing. We obtained 82.09 Gb of clean reads from the 18 samples, with an average of 4.56 Gb of clean data per sample. The average Q20 and Q30 values were 96.92% and 92.32%, respectively. An average of 65.13% clean reads per sample was mapped to the reference genome, and the average number of genes quantified per sample was 19,768.3. The correlation coefficients among duplicate samples at the same time point were all > 0.9. Therefore, we calculated single gene expression as the average expression of all duplicates. We detected 6,583 DEGs generat-

## Paragonimus proliferus infection

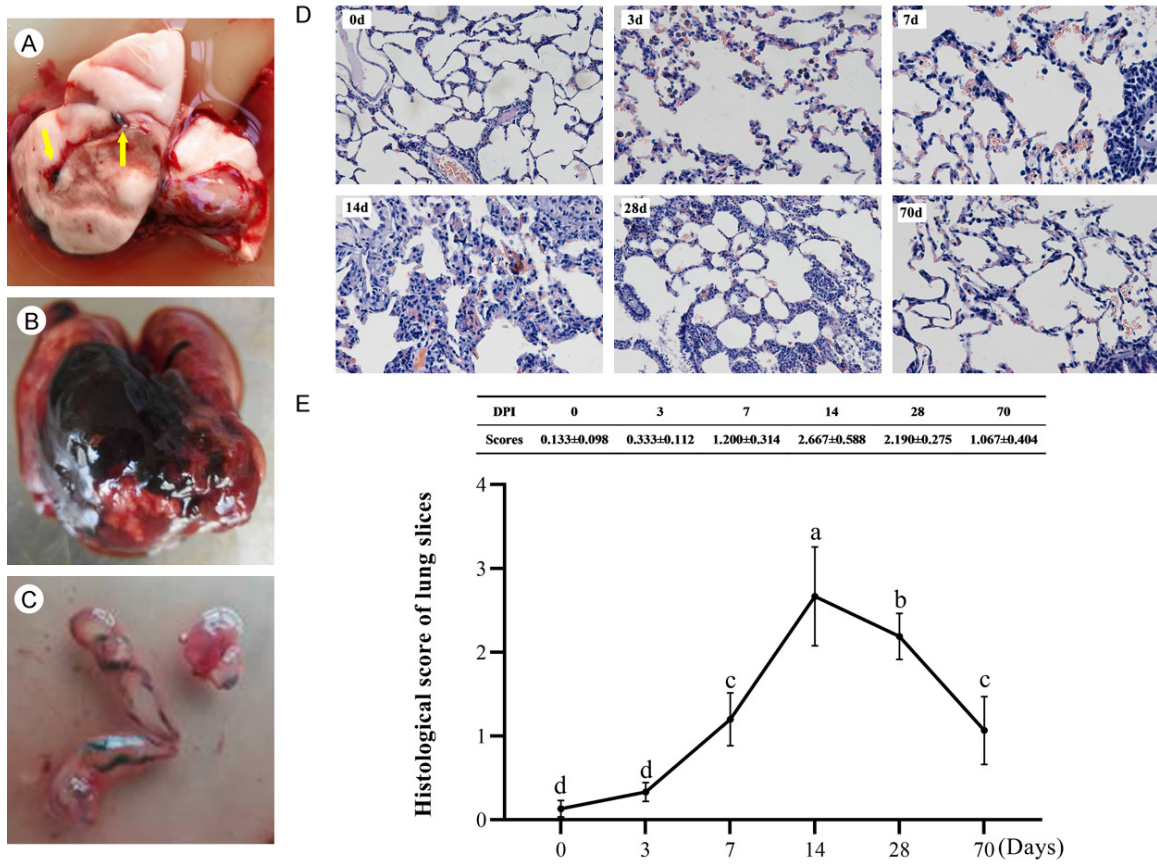


**Figure 1.** Lungs of rats (A and B), *P. proliferus* worms (C), and histological evaluation of rat lung tissues (D and E). (A) Parasitic worms adhere to and drill into lung tissues (yellow arrows). (B) Formation of large cyst to house parasitic worms in rat lung and severe inflammation and necrosis of lung tissues. (C) Adult *P. proliferus* worms isolated from capsules of rat lungs. (D) Rat lung tissues were stained with hematoxylin and eosin ( $\times 400$ ) and evaluated at 0, 3, 7, 14, 28, and 70 days post infection (dpi). 0 d and 3 d: Lung tissues are normal, there is no thickening, swelling or inflammatory cell infiltration of alveolar wall; 7 d: Alveolar walls are slightly thickened and swollen, inflammatory cell infiltration emerges; 14 d: The alveolar walls are severely thickened and swollen, a large number of inflammatory cells are infiltrating, a large range of alveoli collapsed, and the formation of mucus plugs can be seen in the uncollapsed narrow alveolar cavity; 28 d: There are still severe alveolar walls thickening, edema, inflammatory cell infiltration and alveolar collapse, however, the lung tissues injuries has been improved compared with those of 14 d. Meanwhile, some alveolar cavities have been re-inflated, and mucus plugs are reduced; 70 d: Lung damages are significantly recovered, almost to the situation of 3 d or 7 d. (E) Semi-quantitative histopathological analysis of alveolar inflammation in the HE staining of rat lung tissue sections. Letters a, b, c and d in the line chart represent the differences among time points dpi, sharing the same letter at different time points indicates no statistical significance ( $P > 0.05$ ), whereas different letters indicate statistically significant difference ( $P < 0.05$ ).

ed from pairwise comparisons of the six time points mentioned above (Figure 2A).

We used hierarchical clustering (HCL) and PCA analysis based on DEG expression to explore gene expression in the lung tissues of rats parasitized by *P. proliferus* (Figure 2B and 2C). The parasitic process was divided into three stages. The first stage was 0-7 dpi (infection and early parasitism), in which 7 dpi was relatively independent, because cercariae migrated to the lung surface thereafter. The second stage

was 8-28 dpi (mid-parasitism), and the third was 29-70 dpi (post-parasitic). The clustering results corresponded with the visual characteristics of infected rat lung tissues.

### *Paragonimus proliferus* attached to surfaces of rat lung tissues and secreted dsRNA

We clustered 6,583 DEGs into 10 co-expression modules using the K-means algorithm to determine gene expression profiles among the time points. The KEGG and GO enrichment of

## Paragonimus proliferus infection

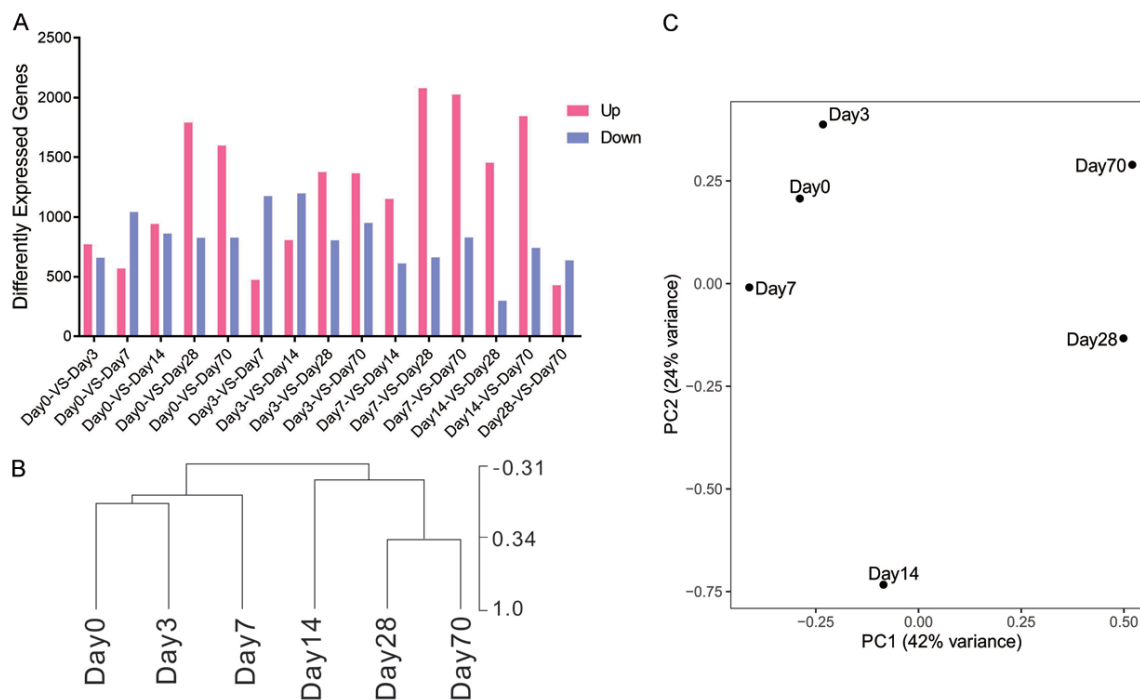


**Figure 2.** Comparative DEG statistics. A. Regulation of DEGs among groups of infected rats ( $n = 3$  per group) determined by sequencing and data analysis. B. Hierarchical clustering of groups according to DEG expression. C. Principal component analysis of groups according to DEG expression.

each module was analyzed and their gene expression and enriched functions were qualified for accuracy. The expression of all genes in each module is represented as averaged z-scores. The expression of significant ( $P \leq 0.05$ ) GO terms was calculated from the annotation results and normalized z-scores of all enriched genes. Correlations between the expression of each module and each GO term were compared using Weighted Gene Correlation Network analysis (WGCNA). Filtering using a correlation coefficient  $\leq 0.05$ , we selected 241 GO Biological Processes terms that were closely correlated with gene expression profiles within each module (Supplementary Tables 1 and 2).

Clustered modules 1, 2, and 4 were abundantly expressed before, or during the early stage of parasitization. Before *P. proliferus* had reached the surface of lung tissues, the rats developed normally for 0-3 days. Most genes in these modules were also enriched in the development of lung tissues, such as module 2, which was significantly enriched in angiogenesis involved in coronary vascular morphogenesis, venous blood vessel development, embry-

onic lung development, and while module 4 was significantly enriched in pulmonary valve morphogenesis, and modulation of the vascular endothelial growth factor receptor (VEGFR) pathway. Genes in module 5 were abundantly expressed only at 7 dpi when *P. proliferus* reached the surface of the lung tissue, and genes were significantly enriched in adhesion of the symbiont to host, cellular response to exogenous dsRNA, necroptotic pathway, and negative signal transducer and activator of transcription (STAT) protein tyrosine phosphorylation regulation (Figure 3). Based on the functional enrichment, *P. proliferus* attached to lung tissues, and then secreted dsRNA that affected the host immune response and signal transduction after reaching the lung surface. *Gbp1*, *Gbp2*, *Gbp4*, *LOC685067*, *Ddx58*, *Ifih1*, and *Tlr3* genes were involved throughout the parasitization process (Figure 4).

Upon parasitizing the surface, *P. proliferus* began to utilize the lung tissues of host. Genes in modules 6 and 7 were abundantly expressed during the mid and late stages of parasitization. Genes in module 6 were significantly enriched in the positive regulation of

## Paragonimus proliferus infection

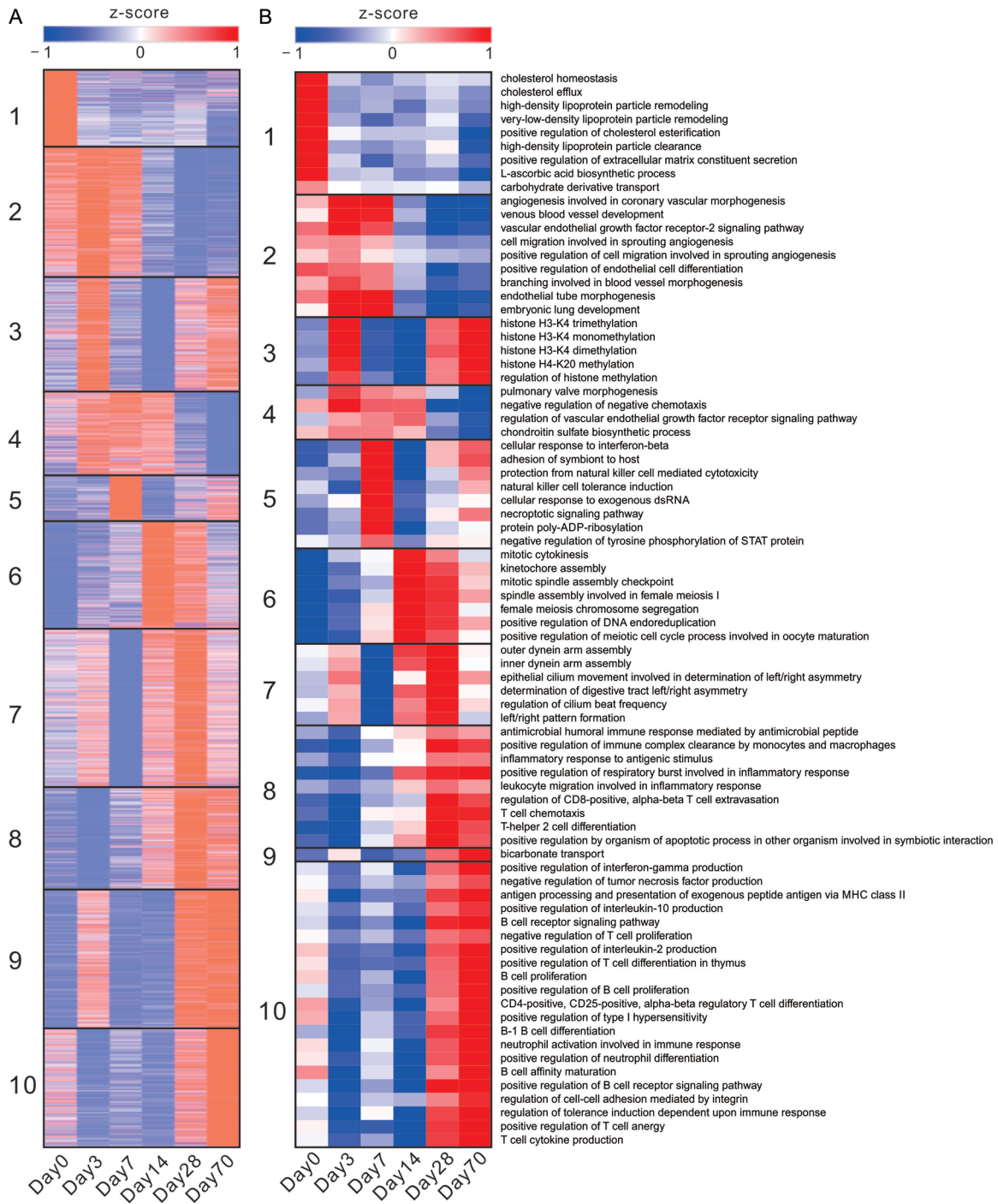


**Figure 3.** K-means heat map of all groups. A. All the DEGs among the time points are clustered into 10 co-expression modules using the K-means algorithm. B. In each of the 10 co-expression modules, the GO functions are enriched by all the DEGs.

DNA endoreduplication, mitotic cytokinesis, and female meiosis chromosome segregation, whereas module 7 was significantly enriched in assembly of the inner and outer dynein arms, digestive tract left/right asymmetry determina-

tion, and the formation of left/right patterns (Figure 3). During the development of *P. proliferus*, mitosis and meiosis proceeded by affecting the expression of associated genes in the lung tissues, which subsequently affected

Paragonimus proliferus infection

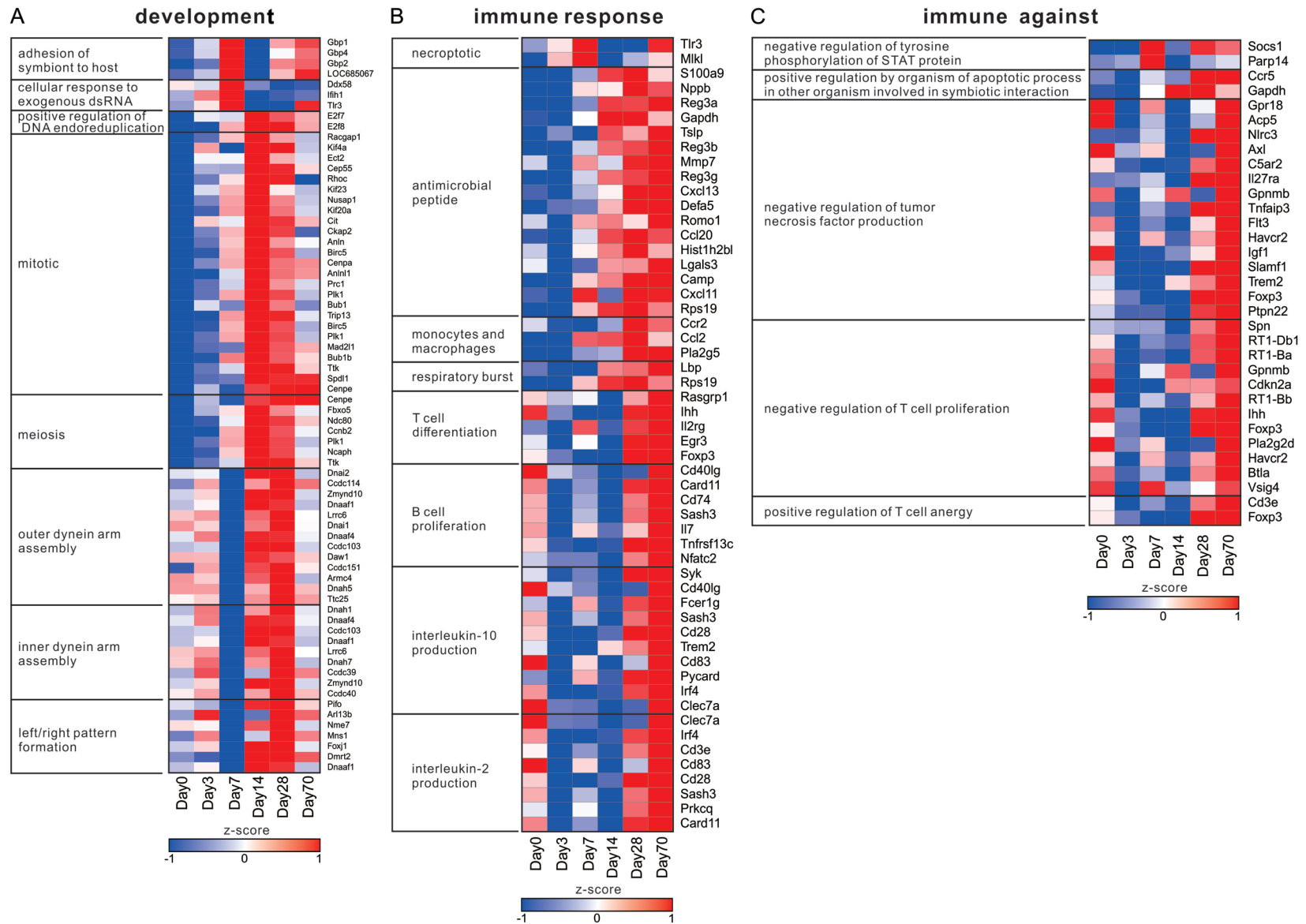


**Figure 4.** K-means heat map and functional enrichment of corresponding gene sets. Three heat maps show corresponding genes based on functions and their enrichment. A-C. Corresponding genes related to development, immune response and immune against, respectively.

the expression of genes associated with dynein arm to develop symmetrical organs in these tissues. We identified 63 genes that mainly participated in the entire process such as *E2f7*, *E2f8*, *Racgap1*, and *Kif4a* (**Figure 4**). The genes in module 7 were also abundantly expressed before *P. proliferus* reached the surface of the lung tissue, as they mainly influenced the development of rat lung tissues.

### *Interactions between P. proliferus and host at various parasitic stages*

After *P. proliferus* reached the surface of the rat lung tissues, different immune pathways became activated at each developmental stage of parasitization. In turn, *P. proliferus* responded in various ways to these strategies. During the early stage, *P. proliferus* cells were necrosed through the necroptotic signaling pathway, while *P. proliferus* resisted activation of the necroptotic signaling pathway by activating the negative regulation of genes associated with STAT protein tyrosine phosphorylation in lung tissues. Module 5 was significantly enriched in the negative STAT protein tyrosine phosphorylation regulation and necroptotic pathways at this point (**Figure 3**). The genes involved in this stage were mainly *Socs1* and *Parp14* (**Figure 4**).

At the mid-parasitism stage, the elimination of monocytes and macrophages, the antibacterial humoral immune response mediated by antimicrobial peptides, and the inflammatory response of respiratory bursts to defend against infection were regulated in the rats. On the other hand, in order to survive in host's lungs, *P. proliferus* altered the expression of genes that were assigned to the GO terms of "positive regulation by organism of apoptotic process in other organism involved in symbiotic interactions". For instance, module 8 was significantly enriched in positive immune complex clearance regulation *via* macrophages and monocytes, function of antimicrobial peptide-mediated antimicrobial humoral immunity, positive respiratory burst regulation related to inflammatory response, and positive organism regulation of the apoptotic process within additional organisms related to symbiotic interactions. In addition, T cells also differentiated in the rats at this time point (**Figure 3**). The main genes involved in the immune response at this stage were *Ccr5* and *Gapdh* (**Figure 4**).

By the post-parasitic stage, T cells and B cells were regulated to defend the rats against infection by *P. proliferus*, which altered the expression of genes associated with negative T-cell growth modulation, positive T-cell disability regulation, and negative tumor necrosis factor generation regulation to reduce immune protection in the rats. For example, module 10 was significantly enriched for positive T-cell energy regulation, positive interleukin-2 generation regulation, positive interleukin-10 secretion regulation, positive B-cell growth, positive T-cell differentiation regulation within the thymus, negative T-cell growth regulation, and negative regulation factor secretion (**Figure 3**). The 29 genes involved in the immune response at this stage mainly included *Gpr18*, *Acp5*, *Nlrc3*, and *Axl* (**Figure 4**).

### *Confirmation by qRT-PCR*

We randomly selected six genes for qRT-PCR analysis to confirm the transcriptome sequencing results (**Figure 5**). All expression profiles of these six genes were validated by qRT-PCR. Most of the gene expression profiles also matched the RNA-Seq data, which verified that our results were reliable.

### **Discussion**

In this study, we analyzed the lung tissues of SD rats infected with *P. proliferus* using dynamic transcriptional profiling for the first time. Most previous studies on *Paragonimus spp.* focused on transcriptome analysis of worms, whereas few focused on infected hosts. We compared dynamic gene expression in infected rats at 3, 7, 14, 28, and 70 dpi with that in control rats (0 dpi) by analyzing RNA sequences based on *P. proliferus* development in the host.

We detected DEGs during each interval, indicating that host gene expression profiles were differentially altered by *P. proliferus* worms during different phases of infection. Based on the different gene expression characteristics, as well as general observation of rats' thorax and lungs and HE staining of lung tissues, for the first time, parasitic process of *P. proliferus* infection was divided into three stages, including early-, mid-, and post-parasitic periods (0-7, 8-28, and  $\geq 29$  dpi, respectively). As is known, *Paragonimus* worms always penetrate into enterocoelia of hosts, keep moving to and pass

## Paragonimus proliferus infection

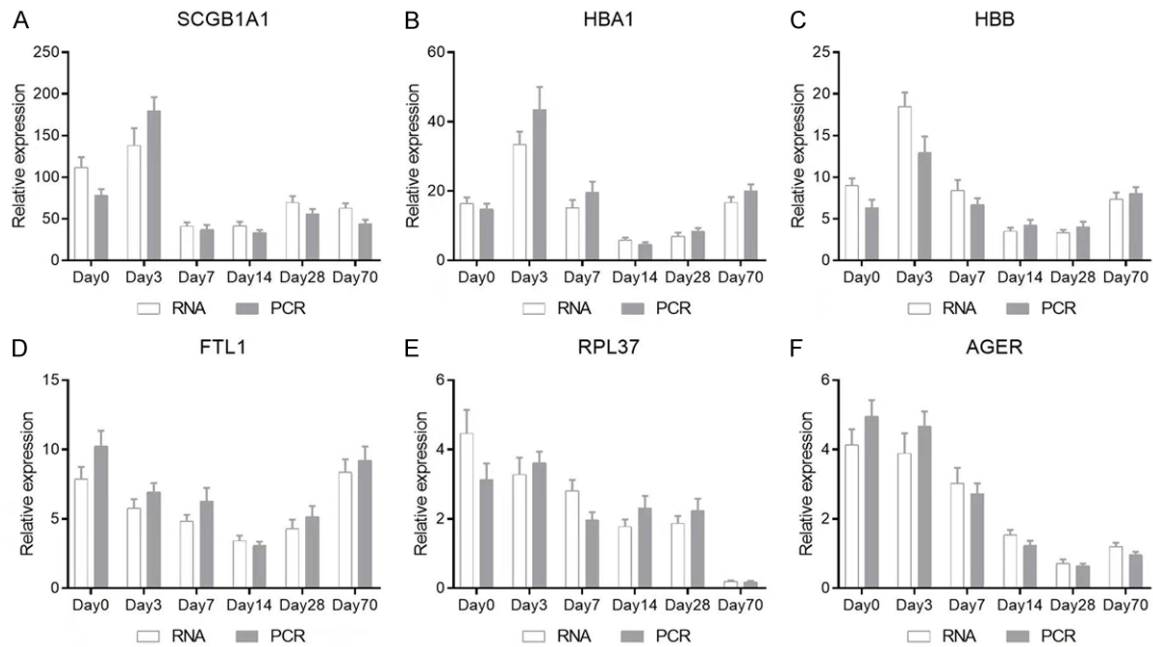


**Figure 5.** Verification of six DEGs by qRT-PCR. Gray and white bars represent relative gene expression determined by qRT-PCR and RNA-Seq, respectively (n = 3 samples/day). A-F. Relative gene expression of SCGB1A1, HBA1, HBB, FTL1, RPL37 and AGER, respectively.

through diaphragm, and then reach to thorax or lungs [19]. Surprisingly, in current study, we found genus *P. proliferus* only spent less than 7 days for such a long journey, which was similar to *P. kellicotti* that was reported to have reached lung parenchyma in cats in the first week after infection [20]. Meanwhile, the lung of rats started to be damaged synchronously with the gradual mature of *P. proliferus* worms, especially on 14~28 dpi. *P. proliferus* takes less than four weeks, which is shorter than previously reported “always two months” in *Paragonimus* and 5~8 weeks in *P. kellicotti* [20-21] to be mature after infection. Worth to note that the maturing of *P. proliferus* and serious lung injuries provides a precondition to diagnosis viably seeking parasite eggs in sputum or faces excreted by infected host, and it becomes the key stage for controlling the condition of such disease.

*Paragonimus spp.*, (pulmonary flukes), are mainly parasitic in the lung tissues of mammals and cause pulmonary fluke disease. For the parasites themselves, colonization into the host is the key for their pathogenicity. In current study, genes of Gbp1, Gbp2, Gbp4 and LOC685067 related to adhesion of symbiont to host were over-expressed at 7 dpi. Similar phe-

nomenon was already observed in *Toxoplasma gondii* infection, in which the host genes of GBP1 and GBP2 played a parasiticidal role and restricted parasite growth [22]. At the time point of 7 dpi during *P. proliferus* infection, the parasite worms only reached the surface of the rat lungs, at where it attempted to colonize and parasitize while the host had to respond accordingly to this foreign invader. Selleck et al. [23] also claimed that Gbp1 gene played important roles in host defense and cell-autonomous control of toxoplasmosis. In a word, we infer that the function related to GO terms of adhesion of symbiont to host plays an essential role in the process of *P. proliferus* paragonimiasis. GO term of cellular response to exogenous dsRNA was also significantly enriched at 7 dpi, indicating that the parasite rapidly releases dsRNA as it reaches the lung surface. Exogenous dsRNA is closely related to the host immune response in helminth diseases. Double-stranded RNAs from a non-viral pathogen can induce the innate immune response of host through TLR3 signalling, for example, dsRNAs from the *Schistosoma* activates TLR3 in Dendritic Cells [24]. Signal of virus infection or exogenous dsRNA can be recognized by TLR3, retinoic-acid inducible gene-1 and melanoma differentiation-associated 5,

coded by *Ddx58* and *Ifih1*, respectively [25]. In current study, high expression of *Ddx58*, *Ifih1* and *Tlr3* in rat lungs, enriched to cellular response to exogenous dsRNA, suggests that, like virus infection, pattern-recognition receptor (PRR) - related signaling were rapidly activated by *P. proliferus* worms once parasites reach the lung surface of host, and the activation of PRRs related signaling may be induced by the secreted dsRNAs from parasite worms.

Furtherly, activation of signal transducer and activator of transcription (STAT) signaling strongly induces type I IFN production [25, 26], such as IFN- $\alpha$ , - $\beta$  and - $\gamma$ , so we infer that enrichment of negative signal transducer and activator of transcription (STAT) protein tyrosine phosphorylation regulation is beneficial to *P. proliferus* avoiding being cleared at the time of parasite reaching the host thorax and keeping survival. *Socs1* and *Parp14* also participated in the process of *P. proliferus* infection at 7 dpi, the former is a feedback regulator of STAT1/3 [27] and the latter has a closely interaction with STAT6 which is critical in activating cytokine gene expression and cytokine signaling in the immune cells and in target tissue cells [28].

We also showed that the *P. proliferus* worms use nutrients derived from lung tissues for mitosis and meiosis, and the dynein arm of lung tissues to develop symmetrical organs. Histopathological changes in rat lung tissues after *P. proliferus* infection showed that rat lung tissues can develop normally after infection.

In current *P. proliferus* infection model, the rats had aggravated disease or even died after 7 dpi, especially during 14~28 dpi. Moreover, functions of T cells, monocytes and macrophages as well as apoptotic process were simultaneously regulated in a wide range, accompanied by antimicrobial humoral immunity and inflammatory response. This strongly suggests that while the host is attempting to eliminate foreign invaders, the elimination process also causes severe inflammation or immune damage to itself. Regulation of host immune cells, including monocyte/macrophage and T/B cells, is common in helminth infection. *Brugia malayi* can drive monocyte dysfunction via induction of indoleamine 2,3-dioxygenase, IFN- $\gamma$ , or autophagy, and increase of M2 phenotype [29]. *Trichinella spiralis* can also inhibit polarization of M1 monocyte/macrophage [30].

Microbicidal functions of host phagocytic cells are always manipulated in order that the pathogen *Leishmania* can survive or proliferate in host, host; meanwhile, pathogen also promotes differentiation of T cells, producing anti-inflammatory cytokines which eventually lead to pathogenesis [31]. Parasite triggers both innate and adaptive immunity in mammal hosts infected with *Trypanosoma brucei*, and macrophages have a microbicidal role as innate defense for trypanosome clearance while lymphocytes, especially T cells, carry out adaptive immune defense [32].

Helminths, including nematodes, cestodes and trematodes, induce lung injuries due to worm migration, host immune activation or systemic inflammatory response, in addition, activation of host immune responses may result in tissues injuries, provide immune tolerance, and protect against the development of disease [33]. Immune response in the late stage of *P. proliferus* infection (from 29 dpi) mainly includes a wide range of positive or negative function regulations on hosts' T or B cells, accompanied by some regulations of IFN- $\gamma$ , TNF or IL-2 related products, as well as antigen processing and presentation of exogenous peptide. The coexistence of negative and positive bidirectional regulation of immune function, on the one hand, causes a certain degree of inflammation or immune damage to the lung tissues; on the other hand, it also appropriately limits the severity of the injury and avoids the strong immune clearance of parasites, which is conducive to the long-term parasitic and survival of parasites, and the formation of chronicity.

We previously published the dynamic transcriptome of *P. proliferus* after infection [34]. This study provides a time-course analysis of *P. proliferus* development in the host and shows that different pathways involved in the colonizing rat lung tissues. However, the pathogenic, immune evasion, and organ targeting mechanisms of infected hosts remain unclear; thus dynamic transcriptional profiling of infected hosts is necessary. Here, we found that different immune reactions were activated according to infection stages. We also analyzed the key genes that corresponding to the response pathways. Although we verified our RNA sequencing findings using RT-qPCR, further studies are needed to define the function of the corre-

sponding genes and develop preventive methods and agents to treat paragonimiasis.

### Conclusions

In the early stage of *P. proliferus* infection, the worms colonize in host by attaching to lung surfaces and secreting dsRNA, and the symbiont adhesion to host and response of host to exogenous dsRNA are regulated. In the middle stage, after the successful colonization, a large amount of innate or adaptive immune relating cells, such as monocytes, macrophages and T cells, are activated, resulting in severe lung injury and even death of the host. In the late stage, coexistence of both negative and positive regulation of immune response causes a certain degree of inflammation or immune damage, and simultaneously limits the severity of disease and avoids the strong immune clearance of parasites, which is conducive to parasitic survival and chronicity of disease.

### Acknowledgements

We thank the residents of Mengla County, Yunnan Province, China for their assistance in collecting local freshwater crabs. This study was supported by the Special Foundation for Basic Research Program of Yunnan Province Science and Technology (Grant No. 202101-AT070054), Yunnan Local Colleges Applied Basic Research Projects (Grant No. 2018-FH001-087), and the Health Research Project of Kunming Health Commission (Grant No. 2020-03-08-113).

### Disclosure of conflict of interest

None.

**Address correspondence to:** Shenghao Li, Clinical-Medical Center of Infectious Disease of Yunnan Province, The Third People's Hospital of Kunming, No. 319 Wu Jing Road, Guan Du District, Kunming 650043, Yunnan, China. Tel: +86-13698705323; E-mail: doctorlee3h@163.com; Wenlin Wang, School of Basic Medicine, Kunming Medical University, No. 1168 West Chun Rong Road, Cheng Gong District, Kunming 650500, Yunnan, China. Tel: +86-13078750561; E-mail: wangwenlin331@163.com

### References

[1] Yoshida A, Doanh PN and Maruyama H. Paragonimus and paragonimiasis in Asia: an update. *Acta Trop* 2019; 199: 105074.

- [2] Blair D, Xu ZB and Agatsuma T. Paragonimiasis and the genus *Paragonimus*. *Adv Parasitol* 1999; 42: 113-222.
- [3] Razeq AA, Watcharakorn A and Castillo M. Parasitic diseases of the central nervous system. *Expert Rev Neurother* 2011; 21: 815-41.
- [4] Singh TS, Sugiyama H, Lepcha C and Khanna SK. Massive pleural effusion due to paragonimiasis: biochemical, cytological, and parasitological findings. *Indian J Pathol Microbiol* 2014; 57: 492-4.
- [5] Blair D. Paragonimiasis. *Digenetic Trematodes*: Springer; 2019. pp. 105-38.
- [6] Amaro DE, Cowell A, Tuohy MJ, Procop GW, Morhaime J and Reed SL. Cerebral paragonimiasis presenting with sudden death. *Am J Trop Med Hyg* 2016; 95: 1424-7.
- [7] Doanh PN, Hien HV, Nonaka N, Horii Y and Nawa Y. Genetically variant populations of *Paragonimus proliferus* Hsia & Chen, 1964 from central Vietnam. *J Helminthol* 2013; 87: 141-6.
- [8] Zhou BJ, Yang BB, Doanh PN, Yang ZQ, Xiang Z, Li CY, Shinohara A, Horii Y and Nawa Y. Sequence analyses of ITS2 and CO1 genes of *Paragonimus proliferus* obtained in Yunnan province, China and their similarities with those of *P. hokuoensis*. *Parasitol Res* 2008; 102: 1379-83.
- [9] Doanh PN, Hien HV, Nonaka N, Horii Y and Nawa Y. Co-existence of *Paragonimus harinasutai* and *Paragonimus bangkokensis* metacercariae in fresh water crab hosts in central Viet Nam with special emphasis on their close phylogenetic relationship. *Parasitol Int* 2012; 61: 399-404.
- [10] Fang LI. Expression and significance of MMP-9 and TIMP-1 in lung fibrosis of rats infected with *paragonimusproliferus*. *China Medicine and Pharmacy* 2018.
- [11] Zhou BJ. Scanning electron microscopy of *Paragonimus proliferus*. *Zhongguo Ji Sheng Chong Xue Yu Ji Sheng Chong Bing Za Zhi* 2005; 23: 288-91.
- [12] Szapiel SV, Elson NA, Fulmur JD, Hunninghake GW and Crystal RG. Bleomycin induced interstitial pulmonary disease in the nude, athymic mouse. *Am Rev Respir Dis* 1979; 120: 893-9.
- [13] Liu Y, Zhang C, Fan J, Xiao L, Yin B, Zhou L and Xia S. Comprehensive analysis of clinical significance of stem-cell related factors in renal cell cancer. *World J Surg Oncol* 2011; 9: 121.
- [14] Zhang T, Cheng G, Sun L, Deng L, Wang X and Bi N. Transcriptome alteration spectrum in rat lung induced by radiotherapy. *Sci Rep* 2019; 9: 19701.
- [15] Liu Y, Bill R, Fiszman M, Rindfleisch T, Pedersen T, Melton GB and Pakhomov SV. Using Sem-Rep to label semantic relations extracted from clinical text. *AMIA Annu Symp Proc* 2012; 2012: 587.

## *Paragonimus proliferus* infection

- [16] Langmead B and Salzberg SL. Fast gapped-read alignment with Bowtie 2. *Nat Methods* 2012; 9: 357-9.
- [17] Lateef A, Prabhudas SK and Natarajan P. RNA sequencing and de novo assembly of *Solanum trilobatum* leaf transcriptome to identify putative transcripts for major metabolic pathways. *Sci Rep* 2018; 8: 15375.
- [18] Harris MA, Clark J, Ireland A, Lomax J, Ashburner M, Foulger R, Eilbeck K, Lewis S, Marshall B, Mungall C, Richter J, Rubin GM, Blake JA, Bult C, Dolan M, Drabkin H, Eppig JT, Hill DP, Ni L, Ringwald M, Balakrishnan R, Cherry JM, Christie KR, Costanzo MC, Dwight SS, Engel S, Fisk DG, Hirschman JE, Hong EL, Nash RS, Sethuraman A, Theesfeld CL, Botstein D, Dolinski K, Feierbach B, Berardini T, Mundodi S, Rhee SY, Apweiler R, Barrell D, Camon E, Dimmer E, Lee V, Chisholm R, Gaudet P, Kibbe W, Kishore R, Schwarz EM, Sternberg P, Gwinn M, Hannick L, Wortman J, Berriman M, Wood V, de la Cruz N, Tonellato P, Jaiswal P, Seigfried T and White R; Gene Ontology Consortium. The Gene Ontology (GO) database and informatics resource. *Nucleic Acids Res* 2004; 32 (Database issue): D258-61.
- [19] Choi DW. *Paragonimus* and paragonimiasis in Korea. *Kisaengchunghak Chapchi* 1990; 28 Suppl: 79-102.
- [20] Stromberg PC and Dubey JP. The life cycle of *Paragonimus kellecotti* in cats. *J Parasitol* 1978; 64: 998-1002.
- [21] Silachamroon U and Wattanagoon Y. *Paragonimiasis*. *Hunter's tropical medicine and emerging infectious diseases*: Elsevier; 2020. pp. 928-31.
- [22] Fisch D, Clough B, Khan R, Healy L and Frickel EM. *Toxoplasma*-proximal and distal control by GBPs in human macrophages. *Pathog Dis* 2022; 79: ftab058..
- [23] Selleck EM, Fentress SJ, Beatty WL, Degrandi D, Pfeffer K, Virgin HWt, Macmicking JD and Sibley LD. Guanylate-binding protein 1 (Gbp1) contributes to cell-autonomous immunity against *Toxoplasma gondii*. *PLoS Pathog* 2013; 9: e1003320.
- [24] Aksoy E, Zouain CS, Vanhoutte F, Fontaine J, Pavelka N, Thieblemont N, Willems F, Ricciardi-Castagnoli P, Goldman M, Capron M, Ryffel B and Trottein F. Double-stranded RNAs from the helminth parasite *Schistosoma* activate TLR3 in dendritic cells. *J Biol Chem* 2005; 280: 277-83.
- [25] Johnston SL, Goldblatt DL, Evans SE, Tuvim MJ and Dickey BF. Airway epithelial innate immunity. *Front Physiol* 2021; 12: 749077.
- [26] Zhang R and Tang J. Evasion of I interferon-mediated innate immunity by pseudorabies virus. *Front Microbiol* 2021; 12: 801257.
- [27] Zhang Y, Jing Z, Cao X, Wei Q, He W, Zhang N, Liu Y, Yuan Q, Zhuang Z, Dong Y, Hong Z, Li J, Li P, Zhang L, Wang H and Li W. SOCS1, the feedback regulator of STAT1/3, inhibits the osteogenic differentiation of rat bone marrow mesenchymal stem cells. *Gene* 2022; 821: 146190.
- [28] Krishnamurthy P and Kaplan MH. STAT6 and PARP family members in the development of T cell-dependent allergic inflammation. *Immune Netw* 2016; 16: 201-10.
- [29] Narasimhan PB, Tariq S, Akabas L, Dorward DW, Nutman TB and Semnani R. *Brugia malayi* microfilariiae induce autophagy through an interferon- $\gamma$  dependent mechanism on human monocytes. *Am J Trop Med Hyg* 2022; 106: 1254-1262.
- [30] Cheng Y, Yu Y, Zhuang Q, Wang L, Zhan B, Du S, Liu Y, Huang J, Hao J and Zhu X. Bone erosion in inflammatory arthritis is attenuated by *Trichinella spiralis* through inhibiting M1 monocyte/macrophage polarization. *iScience* 2022; 25: 103979.
- [31] Singh R, Anand A, Rawat AK, Saini S, Mahapatra B, Singh NK, Mishra AK, Singh S, Singh N, Kishore D, Kumar V, Das P and Singh RK. CD300a receptor blocking enhances early clearance of *leishmania donovani* from its mammalian host through modulation of effector functions of phagocytic and antigen experienced T cells. *Front Immunol* 2021; 12: 793611.
- [32] Dias-Guerreiro T, Palma-Marques J, Mourata-Gonçalves P, Alexandre-Pires G, Valério-Bolas A, Gabriel Á, Nunes T, Antunes W, Fonseca IPd, Sousa-Silva M and Santos-Gomes G. African trypanosomiasis: extracellular vesicles shed by *trypanosoma brucei brucei* manipulate host mononuclear cells. *Biomedicine* 2021; 9: 1056.
- [33] Weatherhead JE, Gazzinelli-Guimaraes P, Knight JM, Fujiwara R, Hotez PJ, Bottazzi ME and Corry DB. Host immunity and inflammation to pulmonary helminth infections. *Front Immunol* 2020; 11: 594520.
- [34] Li SH, Yang YR, Li JY, Wu KL, Chang GJ, Hua LJ, Liu SQ, Xu JJ, Ma ZQ, Shu QH, Wang QQ, Bai BL, Ding J, Li HW, Wang WL and Du YR. Dynamic transcriptome landscape of *Paragonimus proliferus* developmental stages in the rat lungs. *Parasitol Res* 2021; 120: 1627-36.